Turkish Journal of Earth Sciences (Turkish J. Earth Sci.), Vol. 19, 2010, pp. 449–471. Copyright ©TÜBİTAK
doi:10.3906/yer-0907-1 First published online 3 December 2009

Bala (Ankara) Earthquakes: Implications for Shallow Crustal Deformation in Central Anatolian Section of the Anatolian Platelet (Turkey)

ONUR TAN[1], M. CENGİZ TAPIRDAMAZ[1], SEMİH ERGİNTAV[1], SEDAT İNAN[1], YILDIZ İRAVUL[2], RUHİ SAATÇILAR[3], BEKİR TÜZEL[2], ADİL TARANCIOĞLU[1], SALİH KARAKISA[2], RECAİ F. KARTAL[2], SAMİ ZÜNBÜL[2], KENAN YANIK[2], MEHMET KAPLAN[2], FUAT ŞAROĞLU[1], ALİ KOÇYİĞİT[4], ERHAN ALTUNEL[5] & NURCAN MERAL ÖZEL[6]

[1] TÜBİTAK Marmara Research Center, Earth and Marine Sciences Institute, Gebze, TR–41470 Kocaeli, Turkey (E-mail: onur.tan@mam.gov.tr)

[2] MRWS General Directorate of Disaster Affairs, Earthquake Research Department, Lodumlu, TR–06530 Ankara, Turkey

[3] Sakarya University, Department of Geophysics, Esentepe Campus, TR–54187 Sakarya, Turkey

[4] Middle East Technical University, Department of Geological Engineering, TR–06531 Ankara, Turkey

[5] Eskişehir Osmangazi University, Department of Geological Engineering, Meşelik Campus, TR–26480 Eskişehir, Turkey

[6] Boğaziçi University, Kandilli Observatory and Earthquake Research Institute, Çengelköy, TR–34684 İstanbul, Turkey

Received 06 July 2009; revised typescript receipt 15 December 2009; accepted 03 December 2009

Abstract: Central Anatolia is quiet in terms of seismic activity, and rarely earthquakes up to magnitude 5.6 occur in the inner part of the Anatolian block or Anatolian platelet. Southeast of Ankara, the capital city of Turkey, two earthquake sequences with maximum magnitude of 5.6 occurred in 2005 and 2007. We discuss these shallow crustal deformation in the Anatolian platelet, in the light of seismological data from these earthquakes (M_L= 5.6) and their aftershocks. Following the earthquake of December 20, 2007 near Bala town, Ankara, we installed seven temporary stations in the first 24 hours to observe the aftershock activity and these operated for more than 2 months. Approximately 920 aftershocks with magnitudes 5.5>M_L>0.8 were located precisely. This is the first well-observed earthquake activity in the Central Anatolian section of the Anatolian platelet. We also re-analyzed the 2005 Bala earthquake sequence. The distribution of the well-located aftershocks and the focal mechanism solutions of the December 20, 2007 event define NW–SE-oriented right-lateral strike-slip faulting on a possible weak zone, namely the Afşar fault zone, as a result of the internal deformation in the Anatolian platelet. Our analyses seem to indicate that the Bala earthquake sequences are probably related to increasing seismic activity, following devastating 1999 earthquakes in the Marmara region, to the west.

Key Words: Afşar fault zone, aftershock, Coulomb, Central Anatolia, crustal deformation, earthquake

Bala (Ankara) Depremleri: Anadolu Levhasının Orta Anadolu Kesiminde Sığ Kabuk Deformasyonuna Katkılar

Özet: İç Anadolu depremsellik açısından sessizdir ve Anadolu bloğu içinde az da olsa 5.6 büyüklüğüne kadar depremler meydana gelmektedir. Türkiye'nin başkenti Ankara'nın güneydoğusunda 2005 ve 2007 yıllarında maksimum büyüklükleri 5.6 olan iki deprem dizisi meydana gelmiştir. Bu çalışmada, bu depremler ve artçı sarsıntılarından elde edilen sismolojik veriler ışığında Anadolu levhasının sığ kabuk deformasyonu tartışılmıştır. Ankara'nın Bala ilçesinde 20 Aralık 2007 tarihinde meydana gelen depremden sonraki ilk 24 saat içinde bölgeye yedi geçici deprem istasyonu kurulmuş ve yaklaşık 2 ay çalıştırılmıştır. Büyüklükleri 5.5>M_L>0.8 arasında olan yaklaşık 920 arçı sarsıntının hassas lokasyonu yapılmıştır. Bu, Anadolu levhasının Orta Anadolu bölümündeki en iyi gözlemlenebilen deprem aktivitesidir.

Ayrıca 2005 Bala depremleri de tekrar analiz edilmiştir. Çok iyi konumlandırılmış 20 Aralık 2007 depremi artçı sarsıntı dağılımı ve fay düzlemi çözümleri, Anadolu levhasının iç deformasyonu nedeniyle olası bir zayıflık zonunda (Afşar fay zonu) KB–GD yönelimli sağ-yanal doğrultu atımlı faylanmanın meydana geldiğini göstermektedir. Yapılan analizlerde, Bala depremlerinin Marmara Bölgesi'nde meydana gelen 1999 depremleri sonrasında daha doğudaki sismik aktivite artışıyla ilişkili olabileceğini göstermektedir.

Anahtar Sözcükler: Afşar fay zonu, artçı sarsıntı, Coulomb, Orta Anadolu, kabuk deformasyonu, deprem

Introduction

In line with increased funding for earthquake research in Turkey (İnan *et al.* 2007), the TÜBİTAK Marmara Research Center (MRC) Earth and Marine Sciences Institute (EMSI) and the General Directorate of Disasters Affairs (GDDA) Earthquake Research Department (ERD) initiated, with financial support from the State Planning Organization (SPO), a new project to establish the necessary human and equipment infrastructure for rapid aftershock studies in Turkey. The aim is to determine the characteristics and behaviour of destructive earthquakes ($M_w \geq 6.0$) by obtaining detailed aftershock records and GPS measurements. The first real experiment under the scope of this project was done following the December 20, 2007 Bala (Ankara) Earthquake (09:48 UTC, M_L= 5.6). One of the main objectives of this project is immediate deployment of seismology stations after the mainshock in order to observe the earliest aftershock activity. Hence, the first station was deployed 9 hours after the mainshock. Although the earthquake is relatively weak (M_L= 5.6), the team decided to monitor aftershock activities for two reasons: firstly that the earthquake was felt strongly in the Capital City, Ankara which is about 50 km northwest of the epicenter; and secondly that the epicentre area is quite close to the Tuz Gölü (Salt Lake) Fault Zone (TGFZ) which is a major fault zone in the region that has been inactive for a long time (Figure 1).

In this study, we present detailed aftershock analyses of the December 20, 2007 Bala earthquake, and also we re-analyse the moderate size earthquake (M_L= 5.3) that occurred on July 30, 2005 in the same region and its large aftershocks.

Geological Setting

As shown in Figure 1A, the Anatolian platelet (AP) is bounded to the north by the giant North Anatolian Fault System (NAFS) and on the south-southeast by the East Anatolian Fault System (EAFS) (Şengör 1979). The NAFS and the EAFS facilitate the tectonic escape of the Anatolian Block to the west (Şengör & Yılmaz 1981). The western part of the AP shows a transition to the Aegean extensional system (AES). The central area does not host major faults and seems to achieve its tectonic escape by moving westward along the NAFS and EAFS without much internal deformation (Şengör & Yılmaz 1981; Reilinger *et al.* 1997; McClusky *et al.* 2000). The AP contains palaeotectonic structures such as the İzmir-Ankara-Erzincan Suture Zone (İAESZ), the Sakarya Continent (SC) and the Kırşehir Block (KB). Palaeomagnetic studies show that, while anti-clockwise rotation (~25° ccw) is observed east of Kırşehir Block (Figure 1A), neotectonic units in the western part of the Anatolian platelet show ~18° clockwise rotation (i.e. Tatar *et al.* 1996; Platzman *et al.* 1998; Gürsoy *et al.* 1998; Piper *et al.* 2002). However, minor internal deformation includes neotectonic secondary strike-slip faults and extensional basins (Bozkurt 2001). Koçyiğit & Deveci (2008) and Koçyiğit (2009) reported that the direction of the compression in the region was NW–SE until late Pliocene, when a neotectonic regime was initiated controlled by active strike-slip faulting caused by approximately N–S compression. The right- and left-lateral faults trend NW–SE and NE–SW, respectively (Figure 1B). The most important structure is the Tuz Gölü Fault Zone (TGFZ, first named by Beekman 1966) with a mapped length of about 200 km (Koçyiğit & Beyhan 1988; Çemen *et al.* 1999). Görür *et al.* (1984) point out that the TGFZ has been active since the Oligocene, and Gürsoy *et al.* (1998) mention that the TGFZ is a boundary zone between blocks with contrasting deformation. Tatar *et al.* (1996) reported that Central Anatolia shows counterclockwise rotation since the late Eocene and Çemen *et al.* (1999) interpreted that this rotation was probably responsible for the Neogene movement

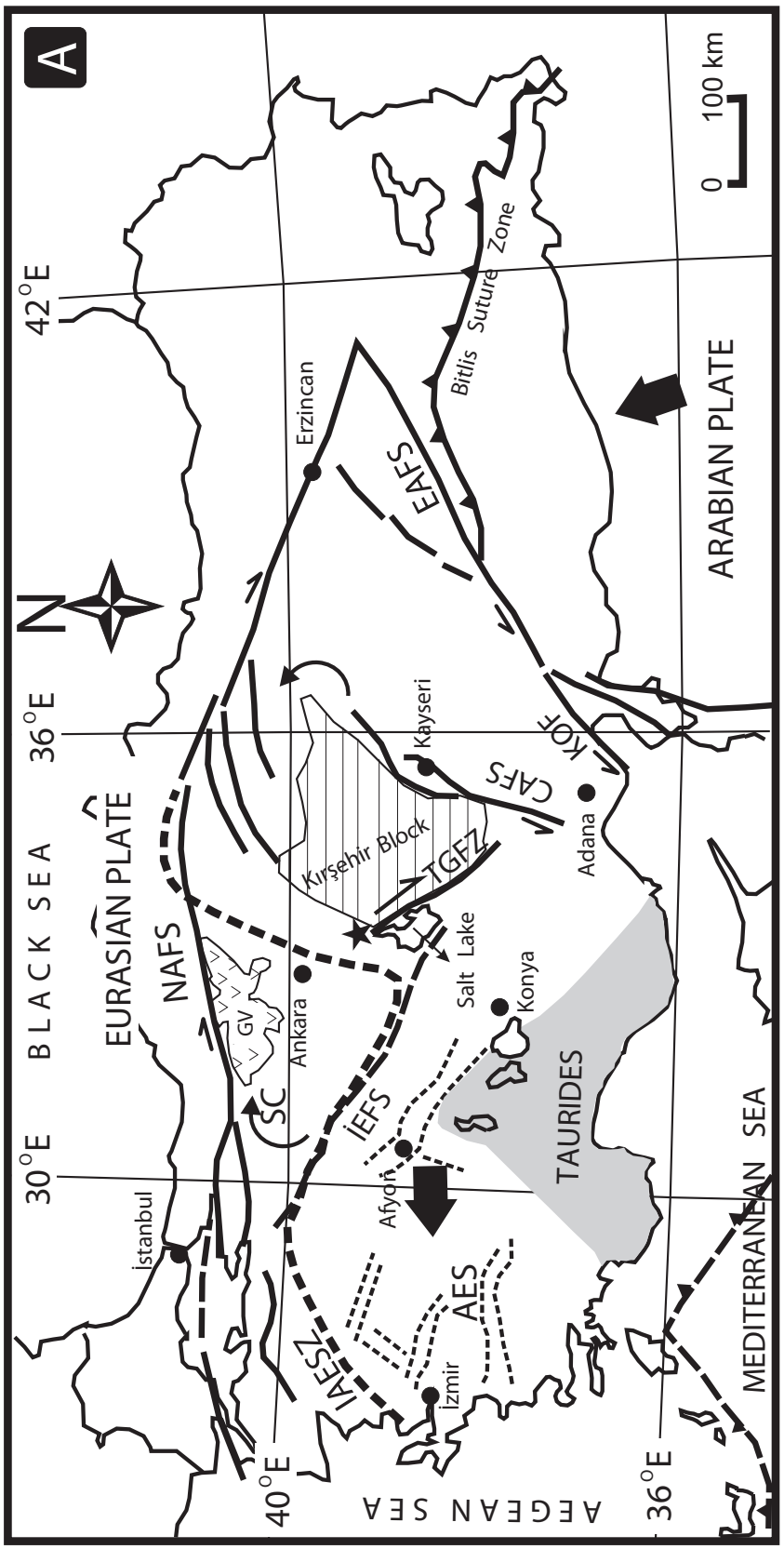

Figure 1. (**A**) Simplified map of the tectonic structures in Turkey (modified from Piper *et al.* 2006). The black heavy arrows show the motion of the plates. The palaeomagnetic rotation directions of the Sakarya Continent and the Kırşehir block are also shown. (**B**) Simplified fault map of the Bala (Ankara) area and its surroundings (modified from Koçyiğit 2009). The stars indicate the epicentre of the Bala earthquakes ($M_L \geq 5.0$). AES– Aegean extensional system, EAFS– East Anatolian Fault System, CAFS– Central Anatolian Fault System, İAESZ– İzmir-Ankara-Erzincan Suture Zone, İEFS– İnönü-Eskişehir Fault System, GV– Galatya volcanics, KOF– Karataş-Osmaniye Fault, NAFS– North Anatolian Fault System, SC– Sakarya Continent, TGFZ– Tuz Gölü Fault Zone.

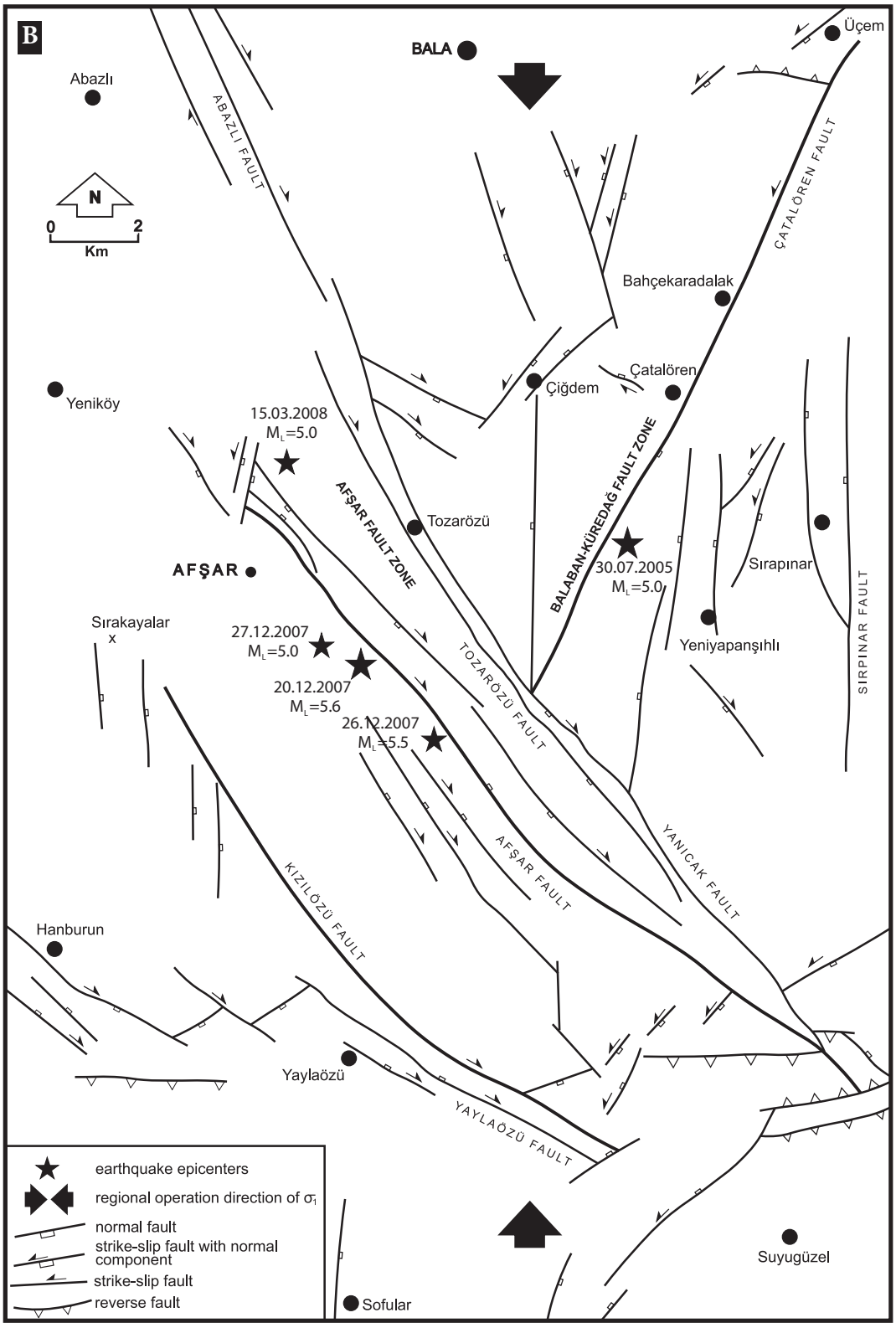

Figure 1. Continued.

along the TGFZ and other northwest-trending faults of the region. One of the main questions is the mechanism of the TGFZ. Şaroğlu *et al.* (1987) observed that the TGFZ is a reverse fault with right-lateral strike-slip component. Beekman (1966) and Koçyiğit & Beyhan (1998) reported that the TGFZ is a right-lateral strike-slip fault zone with a normal slip component. Dirik and Göncüoğlu (1996) remarked that the fault zone consists of parallel to subparallel, normal and oblique right-lateral strike-slip faults displaying a step-like half-graben and horst-graben pattern. On the other hand, Çemen *et al.* (1999) mentioned that the fault may have been formed as a normal fault, suggesting extension or strike-slip faulting with a normal component of movement indicating major transtension at the time of its initiation. However, as all the faults have no important seismological activity (M>4.0–5.0) at present, there is no information about their deep structure in the region. Aydemir (2009) used national earthquake catalogues and interpreted that the area to the south-southeast of the TGZF is completely (seismically) inactive because of the absence of small earthquakes (M<3.0). This interpretation may not be valid because the observation power of the national seismological networks is insufficient to locate the earthquakes M<3.0 in Turkey. Moderate size earthquakes occurring near the TGFZ are thus important as they might reveal clues about possible future activity.

The Bala earthquakes probably occurred on the boundary of the two major palaeotectonic structures (Sakarya Continent and Kırşehir block) and are the first seismic signature, well recorded in the instrumental period. There is no reliable historical earthquake information for this area. The aftershocks of the July 30, 2005 (M_L= 5.3) earthquake, which was the first moderate size earthquake in the region, were recorded only by the national seismic networks. Because of large hypocentral uncertainties (>5 km) and lack of surface deformation, researchers presented different opinions for the mechanism of this seismic activity. Emre *et al.* (2005) mentioned that the earthquake occurred in an area extending NW–SE (~7 km long) and NE–SW (~25 km long) in a right-lateral conjugate fault system. They observed that the main shock occurred on a NE–SW right-lateral strike-slip fault and the aftershocks also concentrated along a NE–SW fault. Kalafat *et al.* (2005) inverted the waveforms from the national seismograph network and found a NE–SW right-lateral strike-slip mechanism (strike 32°, dip 84°, rake 166°, depth 20 km). This solution conflicts with the global moment tensor solutions (i.e. Harvard-CMT, USGS-MT) of the 2005 Bala earthquake but agrees with the NE–SW conjugate faults described by Emre *et al.* (2005). However, Koçyiğit & Deveci (2008) and Koçyiğit (2009) indicated that the earthquake occurred on a NE–SW left-lateral strike-slip fault segment north and northeast of Bala. Detailed analyses of the two earthquake sequences are discussed in the next section, in the hope that they will shed light on the character of the deformation in the region.

Data and Methods

We collected waveforms from the MRC, ERD and the Kandilli Observatory and Earthquake Research Institute (KOERI) broad-band seismic networks for the mainshock. To monitor the aftershocks, seven off-line stations were installed (Table 1, Figure 2), all configured for 100 sps continuous data acquisition. Their locations were chosen according to a good azimuthal distribution and the site structure (bedrock or at least well-compacted soil) within a 30 km radius around the main shock area. They started recording about 12 hours after the main shock and were removed on 28 February 2008. In the observation period, more than 11,000 P- and S-arrivals were handpicked to locate the events.

The hypocentral parameters of the earthquakes were computed with the *Hypocenter* location algorithm described by Lienert & Havskov (1995). The program tries to minimize the time residuals of the phases between observed and theoretical arrival times using a flat-earth layered velocity model. Therefore, accuracy of velocity structure is one of the important parts of location calculations. We tested available models for hypocentral parameters with minimum errors. Two regional studies give detailed velocity structure (Table 2). Toksöz *et al.* (2003) reported a velocity model for the Central Anatolia after an experimental explosion for seismological instrument calibration study near the town of

Table 1. The locations of seismic stations deployed immediately after the December 20, 2007 Bala mainshock. One Güralp 3TD broad-band seismometer is used in Bala town. The other stations have Reftek-130 (R130) recorder with OYO Geospace GS-11D geophone.

Code	Latitude (°N)	Longitude (°E)	Elevation (m)	Town/Village	Instrument
BLA	39.5427	33.1230	1312	Bala	Güralp 3TD
DRP	39.3416	32.7423	1120	Durupınar	R130, GS-11D
BKS	39.1981	33.2628	973	Büyükkışla	R130, GS-11D
CEV	39.4518	33.5685	1020	Üçev	R130, GS-11D
SOF	39.2883	33.0964	958	Sofular	R130, GS-11D
OGB	39.6850	32.8303	1080	Oğulbey	R130, GS-11D
YAR	39.1703	32.9270	1170	Yaraşlı	R130, GS-11D

Keskin, ~50 km NE of Bala. The model has a top layer with V_p= 5.0 km/s P wave velocity and contains gradually increasing velocities. The other model presented by Ergin *et al.* (2003) after a study in a soda mine area near the town of Kazan (~90 km N of Bala). They used the *velest* algorithm of Kissling *et al.* (1994) and described four crustal layers. The top layer of the model has a slow P-wave velocity, generally representing the sediments in the area. There are two other velocity boundaries at 6 and 20 km depth. The model given by Ergin *et al.* (2003) provided better time residuals at the stations and generated lesser uncertainties in the location parameters. The average seismic velocity of the uppermost two layers (sediments) in this model agrees well with 2D seismic prospecting data (Aydemir & Ateş 2006). The shear-wave velocities (V_s) are calculated by the ratio V_s= V_p/1.73. Average time residuals for aftershocks (RMS) should be less then 0.3 s in the inversion location.

Calculation of local Richter magnitude (M_L) is one of the important points that must be mentioned here. Although 4.5 Hz geophones are easy to install in the rupture zone quickly, they are difficult for magnitude calculations because of their narrow frequency response and high damping ratio. Amplitudes of earthquake waveforms sensed by geophones decrease rapidly and waveform durations become extremely short compared to broad-band seismometer records. So, we did not find any aftershock coda-duration magnitudes exceeding 3.0. In order to calculate local magnitudes (M_L), we arranged a methodology by using the *Seismic Analysis Code* (Goldstein *et al.* 1998). First, the sensor and digitizer responses are separated from the velocity records. Then, each waveform is convolved with the Wood-Anderson seismometer response to generate displacement record. The maximum zero-to-pick horizontal amplitude was selected and M_L was calculated for each station. The minimum and maximum extreme values (larger than standard deviation) were removed and the remaining magnitudes were averaged for that event. In fact, the maximum amplitude at a station does not project real value for M_L because the recorded waveforms do not contain low frequencies (i.e. 1 Hz). Nevertheless, this is the only way to approximate the magnitudes of the aftershocks. The magnitudes of the selected large aftershocks which occurred during the survey were compared with values in the national networks (Table 3). Although the coda-duration magnitudes from geophone records (this study-m_d) were too

Table 2. The crustal seismic velocity models for the region. Models A and B were reported by Toksöz *et al.* (2003) and Ergin *et al.* (2003) respectively. In this study, model B was accepted. h and V_p indicates layer thickness and P-wave velocity, respectively. The shear-wave (V_s) velocities were calculated by $V_s = V_p / 1.73$ ratio.

Model - A		Model - B	
h (km)	V_p (km/s)	h (km)	V_p (km/s)
0 – 5	5.0	0 – 1	2.5
5 – 10	5.5	1 – 6	5.7
10 – 20	6.1	6 – 20	6.1
20 – 36	6.4	20 – 33	6.8
36–	7.8	33 –	8.0

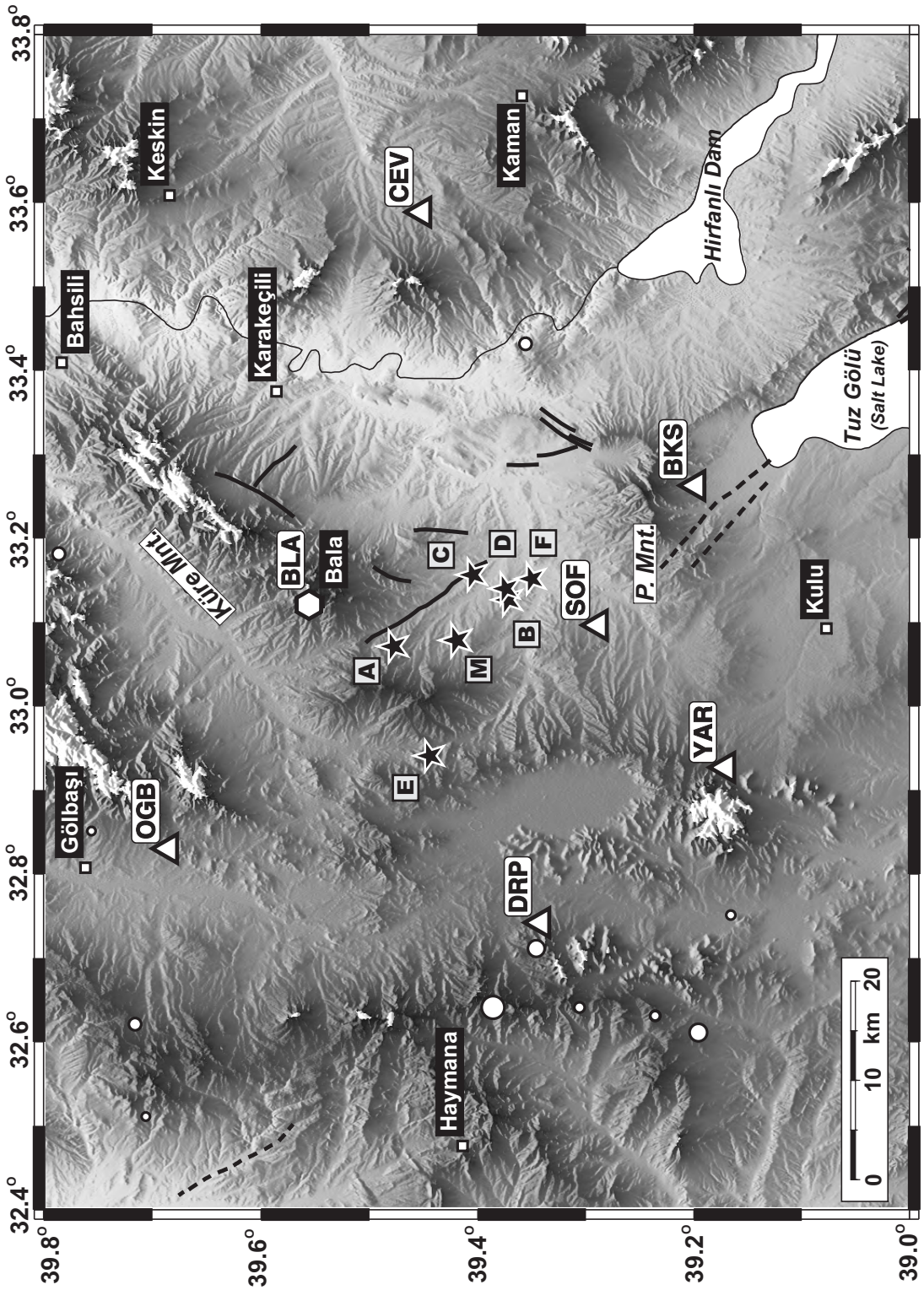

Figure 2. The stations for aftershock study of the 2007 Bala Earthquake. Triangles are the stations with Reftek-130 recorders and geophones (see Table 1). The single Güralp-3TD broad-band station (BLA) is shown with white hexagonal. The mainshock (M) and foreshocks (A-F) are plotted with stars (see Table 3). The white circles represent earthquake (1990–2005, $M \geq 3.0$) locations from the USGS-NEIC catalogue. The active faults (Şaroğlu *et al.* 1992) are shown with black lines. *P.Mnt.*– Paşadağ Mountain.

Table 3. Comparison of the magnitudes reported by different agencies for selected aftershocks. The ERD and KOERI calculate the magnitudes from national broad-band seismology stations. The values in this study are from the temporary aftershocks observation stations which were equipped with geophones.

Date (dd.mm.yyyy)	Time (hh:mm)	This Study		ERD		KOERI	
		m_d	M_L	m_d	M_L	m_d	M_L
26.12.2007	23:47	3.8	5.5	5.3	5.5	–	5.5
27.12.2007[a]	13:47	2.9	5.0	4.9	5.0	–	4.8
27.12.2007[b]	17:56	3.3	4.3	4.2	4.3	–	4.0
01.02.2008	09:11	2.5	4.4	-	4.4	–	4.1

small, as expected, there was no significant difference between the local magnitudes (M_L). Based on our approach, the local magnitudes of the aftershocks were calculated to be between 0.8 and 5.5.

Although we tried to minimize the errors of location parameters, several factors such as network geometry, phase reading quality and crustal structure uncertainties limited our endeavours. Relative earthquake location methods can improve absolute hypocentre locations. For this purpose, we used a double-difference algorithm (*hypoDD*) developed by Waldhauser & Ellsworth (2000). The *hypoDD* algorithm assumes that the hypocentral separation between two earthquakes is small compared to the event-station distance and the scale length of velocity heterogeneity, so that the ray paths between the source region and a common station are similar along almost the entire ray path. If so, the difference in travel times for two events observed at one station can be accurately attributed to the spatial offset between the events (Fréchet 1985; Got *et al.* 1994; Waldhauser & Ellsworth 2000). By linking hundreds or thousands of earthquakes together through a chain of nearby shocks, it is possible to obtain high-resolution hypocentre locations over large distances without the use of station corrections. Two inversion approaches are used in a standard *hypoDD* analysis. The singular value decomposition (SVD) method is very efficient for the well-conditioned systems which have small earthquake clusters (~100 events). However, because of the large size of our data and unknown parameters for the large cluster (more than 200 events), SVD cannot be used effectively and the conjugate gradient algorithm (LSQR), which solves the damped least-squares problem, was selected to save computer memory usage, computation time and efficiency of the algorithm (see Waldhauser & Ellsworth 2000 for details). After relocating the hypocentres, horizontal and vertical error assessment must be done carefully. Unfortunately SVD gives proper least square errors, LSQR reports underestimated errors and these errors must be reviewed by statistical resampling methods and by relocating small subsets of events using SVD mode.

We also read P-wave first motion polarities to find out focal mechanism solutions of the mainshock and the large aftershocks ($M_L \geq 4.0$). All available polarities from national seismic stations and the aftershock network were read carefully and ambiguous polarities were never added to the solutions. The takeoff angles were calculated according to the same velocity structure used for the location determination. The possible nodal planes which agree with the first motion polarities were searched, running the *focmec* program (Snoke *et al.* 1984). No polarity error is allowed in the solutions. Events with multiple acceptable solutions indicating different mechanism or with faulting parameters uncertainties exceeding ±20° were not reported in this study.

Because of the good data set for the 2007 Bala earthquake and its aftershocks, we tried to apply Coulomb failure stress change analyses to understand the stress change in the region caused by the earthquakes. We followed similar methods to those described in King *et al.* (1994) and Stein *et al.* (1997) and used the program *Coulomb 3.0* (Lin & Stein 2004; Toda *et al.* 2005). We assumed an elastic

half-space with a shear modulus of 3.2×10^{11} dyne·cm^2 and Poisson's ratio of 0.25 in calculations. In this exercise a fault friction of 0.4 was assumed.

Earthquake Sequence

The mainshock of December 20, 2007 was recorded by the ERD national broad-band seismic network and the preliminary location was reported as 39.417°N 33.045°E. We collected waveforms from more than one hundred national stations from the ERD and KOERI, and re-read the P and S phases to re-locate the mainshock more precisely. We calculated the Bala main shock coordinates as 39.431°N 33.088°E with minimum horizontal error (±2 km). The new location is about 4 km east of the preliminary reported location. The hypocentre depth is 4.4±2 km. The main shock was preceded by six events in the two hours before the main shock (Table 4, Figure 2). Although the magnitudes of the foreshocks ($2.8\leq m_d\leq3.6$) are not large enough and the station distribution is sparse, their locations agree well with the aftershock distribution described in the next section. The first event (A) occurred at the north end of the region and the next four events (B, C, D and F) were in the south. Only one event (E) was far from the activity area.

We located 923 aftershocks occurring in 71 days with the *Hypocenter* algorithm. The horizontal and vertical location errors are 1–2 and 1–3 km respectively and the average station time residuals (RMS) are 0.15 seconds. The aftershocks occurred in an approximately 20×5 km narrow band trending NW–SE. To improve the hypocentre locations with *hypoDD* analysis, we preprocess in order to select data from connected earthquakes to build a network of links between event pairs. The maximum hypocentral separation was chosen as 2 km. The minimum number of phases for an event-pair to be recorded at a common station is defined as 8, which is the minimum value to solve unknown parameters of pairs (6 for space and 2 for time). Several inversions are executed with different model parameters to find a stable solution. We could relocate 706 aftershocks precisely. 217 events were excluded in inversion. 68 of them are very shallow events (~1 km) with poor vertical control. The other 149 events have also poor links with neighbouring events and cannot be used in the iterations. The relocated events are shown in Figure 3. The uncertainties of the hypocentre locations after *hypoDD* (LSQR) analyses are tested with two different methods. First we select highly correlated event-pairs which represent three different parts in the aftershock area. These sub-clusters are shown in Figure 3 with the letters N, C and S which refer to the north, centre and south sub-clusters respectively. Each selected event-pair has P and S phase data from at least 5 common stations and has 20 neighbouring event-pairs to form a good continuous chain. The number of events in each sub-cluster and their horizontal and vertical errors are given in Table 5. SVD analysis of *hypoDD* shows the maximum horizontal uncertainty is about 400 m and the vertical errors are little more than 700 m. Our second test is based on a statistical approach. We use the same initial catalogue data and inversion parameters in the final LSQR solution. We add random numbers

Table 4. The foreshock parameters of the December 20, 2007 Bala Earthquake reported by the ERD.

Event	Date (dd.mm.yyyy)	Time (hh:mm)	Latitude (°N)	Longtitude (°E)	Depth (km)	Magnitude (m_d)
Foreshock A	20.12.2007	07:36	39.4698	33.0732	7	3.6
Foreshock B	20.12.2007	07:51	39.3747	33.1142	6	3.2
Foreshock C	20.12.2007	08:12	39.4043	33.1433	7	2.8
Foreshock D	20.12.2007	08:18	39.3763	33.1180	7	3.1
Foreshock E	20.12.2007	08:27	39.4398	32.9462	7	2.8
Foreshock F	20.12.2007	08:57	39.3542	33.1430	6	3.3

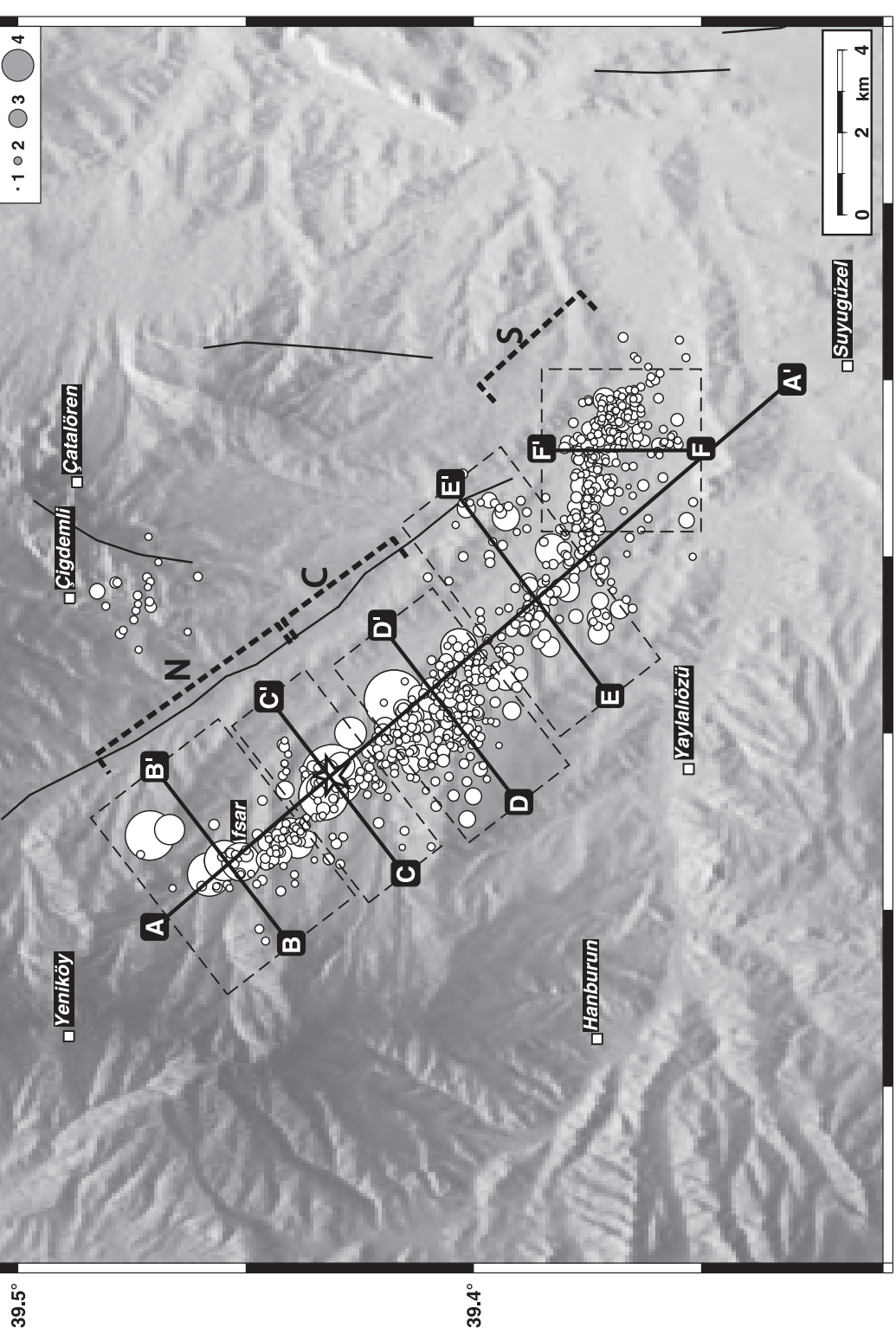

Figure 3. The aftershock locations of the 2007 Bala Earthquake after *hypoDD-LSQR* analysis. N, C and S refer to northern, central and southern subclusters used in *hypoDD-SVD* location error assessment tests respectively (see text for details). The letters (A–F) refer to the depth section profiles are shown in Figure 6. The dashed lines are the event selection area of each profile.

Table 5. The horizontal (E_{xy}) and vertical (E_z) errors of the highest correlated events before and after SVD analyses in *hypoDD*. The earthquakes were selected from the three sub-clusters of the Bala aftershocks (Figure 3A). N– North, C– Centre, S– South.

Region	Number of Events	Before *hypoDD* (m)		After *hypoDD* (m)	
		E_{xy}	E_z	E_{xy}	E_z
N	90	±1500	±2800	< ±400	< ±700
C	130	±1600	±2200	< ±300	< ±700
S	134	±1500	±2000	< ±200	< ±500

between ±1 km to the initial absolute locations in X, Y and Z directions. This allows us to shift the hypocentre location in space and re-link events randomly. After inversion, the location shift of each event is calculated. The process is repeated several times and 1000 well-conditioned inversion solutions are collected. Approximately 175000 samples are acquired to see the statistical distribution. The outliers in the data set are removed using the interquartile range (IQR) method. More than 95% of the total samples remain after the IQR analysis. The dataset represents a normal distribution and the 95% confidence interval (±2σ) shows location variation interval according to the different initial models (Figure 4). This test shows latitudinal, longitudinal and vertical location changes are not more than ±230 m, ±260 m and ±550 m respectively.

The aftershock zone developed quickly and 45% of the total 923 recorded events occurred in the first 10 days. Another 45% of them occurred in January and then the number decreased dramatically in the last month of the observation. Although the aftershocks align along a NW–SE narrow zone (i.e. A-A' profile), the events shift eastwards in the southern (S) segment. Moreover, another small cluster with a few events occurring on the 54th and 55th days of the sequence was seen in the NE of the area (near Çiğdemli village). The aftershock temporal behaviour is given in Figure 5, according to the locations on the A-A' profile in Figure 3. The mainshock occurred in the northern part (~6 km) of the cluster and the first sub-cluster activity occurred in the SE (~13–16 km) for a few days. After December 26, further activity began in the central segment (~8–10 km) and also in the northern part. However, the large aftershocks occurred close to the mainshock and north of it (around Afşar village). These events, especially occurring after January 1, were not followed by smaller events. However, a few tremors form small groups in the southern part (arrows in Figure 5). This can be interpreted as the asperities on that segment being unable to release its energy with a single (relatively large) event, and so generating several micro-earthquakes in a short time. The spatiotemporal distribution of the Bala aftershocks indicates that the northern and southern parts of the deformation area may have different asperity properties. Although the northern part has strong asperities which release its energy in moderate and small events, the southern part contains several small and weak asperities which generate micro-earthquakes only.

The depth section of the sequence shows that the earthquakes occurred between 3 and 9 km deep (Figures 3 & 6A). No event is deeper than 14 km. Those events that especially occurred near the mainshock and north of it align within a very narrow band. The depth sections of these parts show that large aftershocks occurred on a vertical plane which may indicate strike-slip fault segments (Figure 6B, C). However, there are many more events in central part and they scatter across a wider area within the central part (Figure 6D). The southernmost sub-cluster is elongated in an approximately E–W direction and events concentrate at 4–6 km depth (Figure 6F). Deeper aftershocks (8–10 km) were also observed in this segment.

Fault Mechanisms and Stress Changes

We collected all available digital records from the national seismograph networks of ERD and KOERI to read the P-wave first motion polarities of the 2005 and 2007 Bala earthquakes ($M_L \geq 4.0$). The parameters of the earthquakes are summarized in Table 6 as location, local Richter magnitude and faulting parameters. The strike, dip and rake angles of assumed fault plane and the number of P-wave first motion polarities are shown in the following columns. The rupture area is necessary to calculate

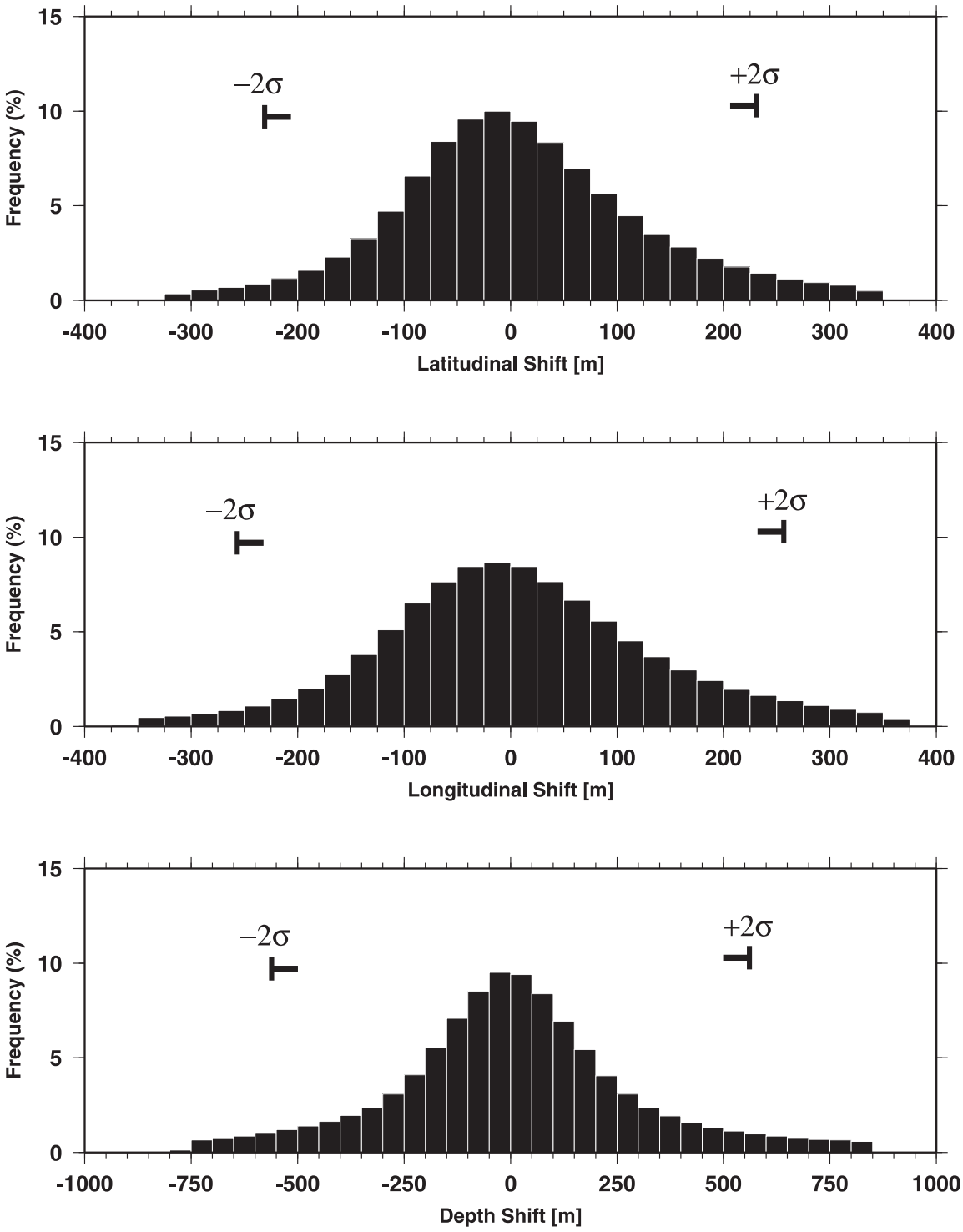

Figure 4. Statistical distribution of event shifts after *hypoDD-LSQR* inversions with different initial locations. Each histogram contains about 95% of total samples (~175000). The ±2σ (two times of standard deviation) lines shows 95% confidence interval.

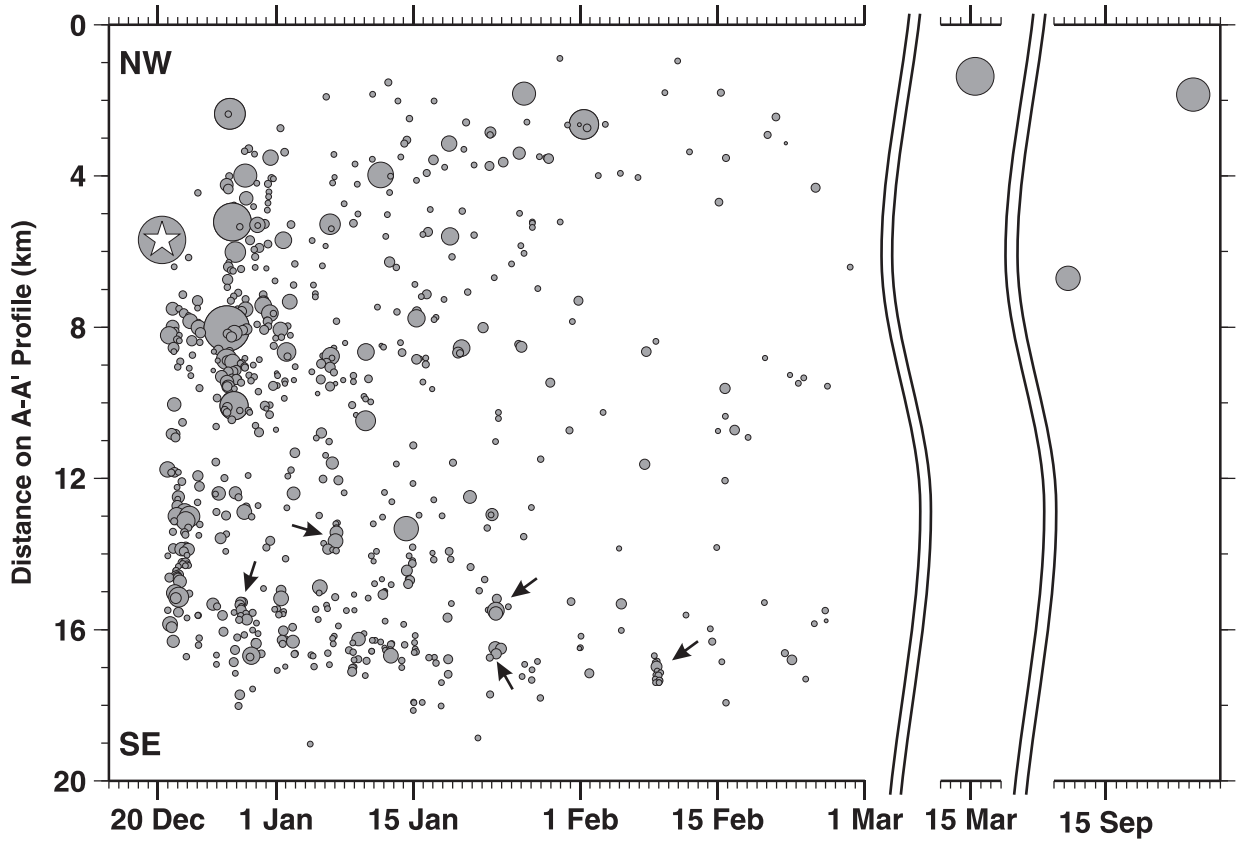

Figure 5. Temporal behaviour of the aftershocks in 2007 and 2008. The locations of the events are plotted according to the A–A' profile (NW–SE) in Figure 3. The large aftershocks occurred close to the mainshock and north of it while the micro-earthquakes form small groups in the southern part. The star is the mainshock (20 December 2007). The arrows are examples for the small micro-earthquake groups in the southern segment.

the Coulomb failure stress change. Therefore, we tried to determine the size of the rupture area (L×W) and average displacement over the fault surface (D_{av}) using the generalized assumptions mentioned in several studies (i.e. Wells & Coppersmith 1994; Mai & Beroza 2000; Tan & Taymaz 2005, 2006). The fault plane solutions of 14 events with P-wave first motion polarities are shown in Figure 7. The focal spheres are plotted in lower hemisphere projection and compressional quadrants are shaded. The available polarities constrain the nodal planes very well and the uncertainties are less than ±5° for most of the solutions.

The 2005 Bala earthquake has no surface rupture and has no reliable aftershock record. The only available data set was from the national seismological networks in Turkey. The large range of the location uncertainties of the small events (m_d= 3.0–4.0) in the national catalogues (> 5 km) pose difficulties in interpretation of the aftershock data for such a small area. So, we tried to relocate the 2005 mainshock and its eight aftershocks to clarify the deformation in the region (Table 6, Figure 8), based on the raw waveforms. The waveforms from the two national networks were collected and the phases were re-read to discover a better location than that reported in the catalogues. The phase readings from the special broadband networks of KOERI in Gölbaşı (50 km NW) and Keskin (50 km NE) were also used. The average location errors of these relocated nine earthquakes barely exceed ±2 km. The mainshock (#1) and its first large aftershock (#2) occurred in the

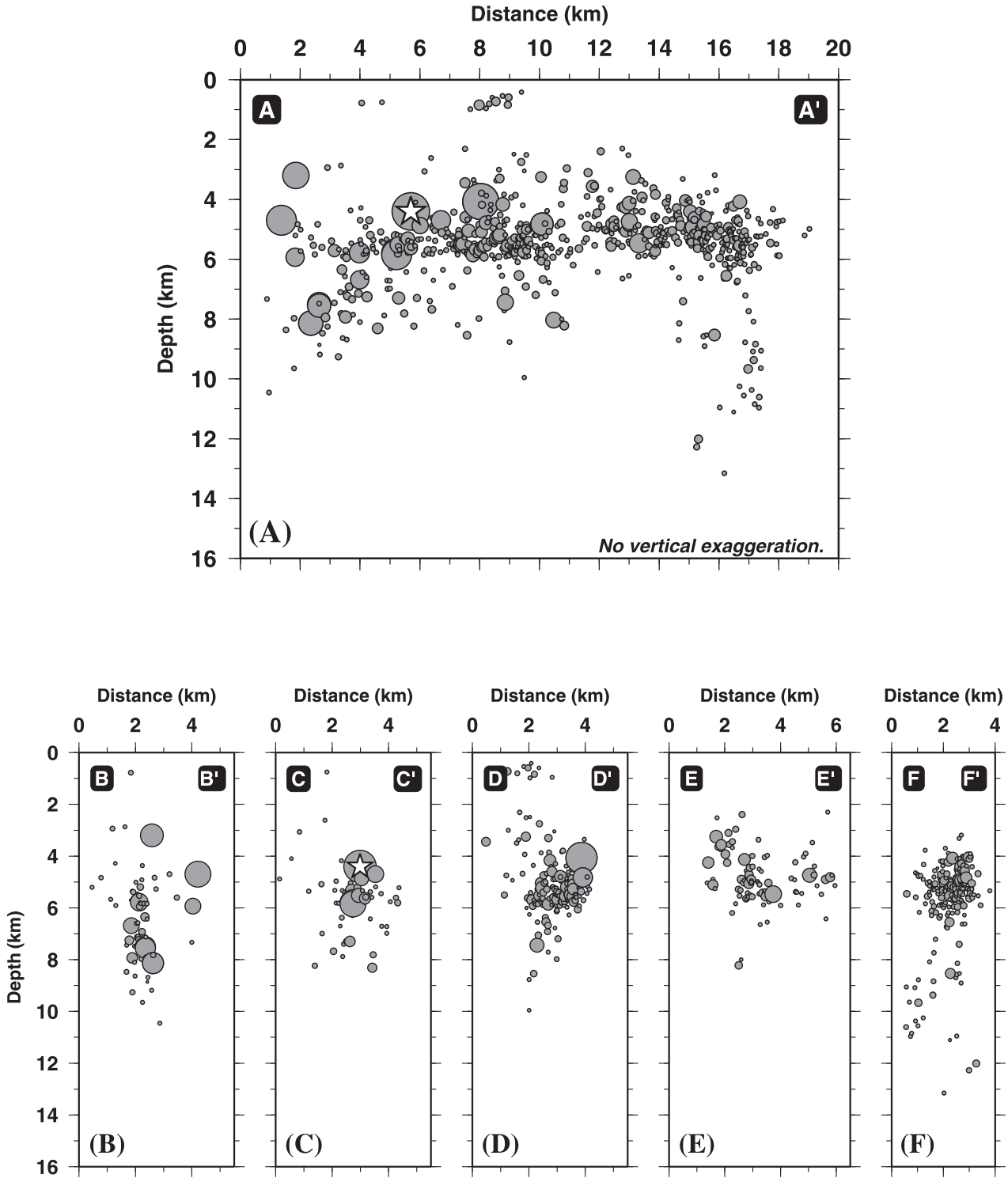

Figure 6. Depth sections of the aftershocks of the December 20, 2007 Bala earthquake. The locations of the profiles are shown in Figure 3B. The star is the mainshock hypocentre. The main activity seems to be confined to 3 to 9 km depth interval.

Table 6. The parameters of the Bala earthquakes ($M_L \geq 4.0$) occurred in 2005, 2007 and 2008. See the text for details. The location parameters after *hypoDD* analyses are marked with asterisks (*). Joint first motion polarity solutions of micro-earthquake groups are marked with letters A–D and average parameters are given.

No	Date (dd.mm.yyyy)	Time (hh:mm)	Latitude (°N)	Longtitude (°E)	Depth (km)	Number of Stations	M_L	Fault Plane Solution			Num. Polarity	W×L (km^2)	D_{av} (cm)
								Strike (°)	Dip (°)	Rake (°)			
	2005												
#1	30.07.2005	21:45	39.452	33.157	5.0	43	5.3	24	72	26	46	4×4	17
#2	31.07.2005[a]	00:45	39.454	33.166	4.2	42	4.2	340	64	180	22	2×2	5
#3	31.07.2005[b]	15:18	39.436	33.138	3.8	64	4.3	17	70	5	29	2×2	5
#4	31.07.2005[c]	15:23	39.439	33.140	4.6	60	4.2	–	–	–	–	–	–
#5	31.07.2005[d]	23.41	39.427	33.123	5.0	79	4.8	24	80	-5	35	3×3	10
#6	01.08.2005[a]	00:45	39.408	33.093	3.0	65	4.6	310	71	175	29	3×3	10
#7	01.08.2005[b]	02:02	39.400	33.118	3.5	45	4.0	120	80	-170	23	2×2	5
#8	01.08.2005[c]	13:22	39.400	33.133	3.6	43	4.6	115	80	175	24	3×3	10
#9	06.08.2005	09:09	39.376	33.143	3.3	56	4.6	–	–	–	–	–	–
	2007–2008												
#10	20.12.2007	09:48	39.431	33.088	4.4	109	5.6	125	85	175	103	6×6	25
#11	26.12.2007	23:47	39.417*	33.109*	4.0*	114	5.5	122	84	-175	117	6×6	25
#12	27.12.2007[a]	07:47	39.455*	33.064*	8.1*	33	4.5	–	–	–	–	–	–
#13	27.12.2007[b]	13:47	39.433*	33.082*	5.8*	107	5.0	155	60	-130	46	4×4	17
#14	27.12.2007[c]	17:56	39.403*	33.124*	4.8*	45	4.3	–	–	–	–	–	–
#15	01.02.2008	09:11	39.451*	33.064*	7.5*	41	4.4	325	81	170	31	2×2	5
#16	15.03.2008	10:15	39.471	33.071	4.7	38	5.0	130	90	175	29	4×4	17
#17	11.09.2008	08:33	39.427	33.100	4.7	32	4.0	320	47	-150	16	2×2	5
#18	23.09.2008	09:09	39.458	33.060	3.2	52	4.7	310	80	170	40	3×3	10
	Joint Solutions (average values)												
A	20–27.12.2007 *(24 events)*		39.39	33.13	5	–	1.7-2.4	210	80	10	98	–	–
B	21–28.12.2007 *(10 events)*		39.38	33.15	5	–	1.8-2.3	5	55	-65	51	–	–
C	14.01.2008 *(5 events)*		39.37	33.17	6	–	1.9-2.9	25	75	-60	27	–	–
D	8–9.02.2008 *(13 events)*		39.36	33.18	5	–	1.6-2.1	325	55	-90	48	–	–

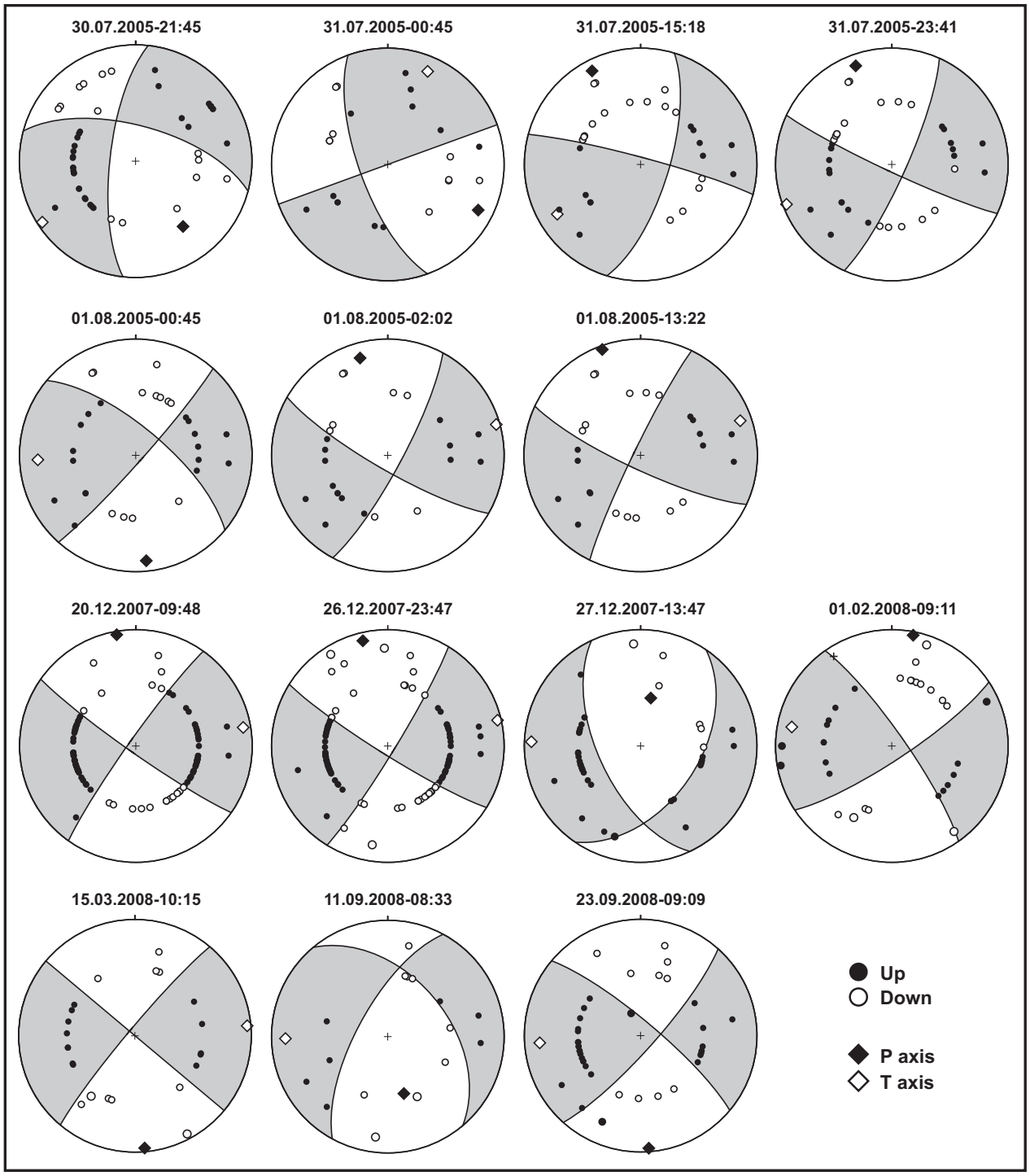

Figure 7. P-wave first motion polarities of the 2005 and 2007 Bala mainshocks and their large ($M_L \geq 4.0$) aftershocks. The event dates and origin times are given above the focal spheres (see Table 6). The compressional quadrants are shaded in grey. The black and white circles refer to up and down P-wave first motion polarities respectively. P and T axes are also represented by the solid and open diamonds respectively.

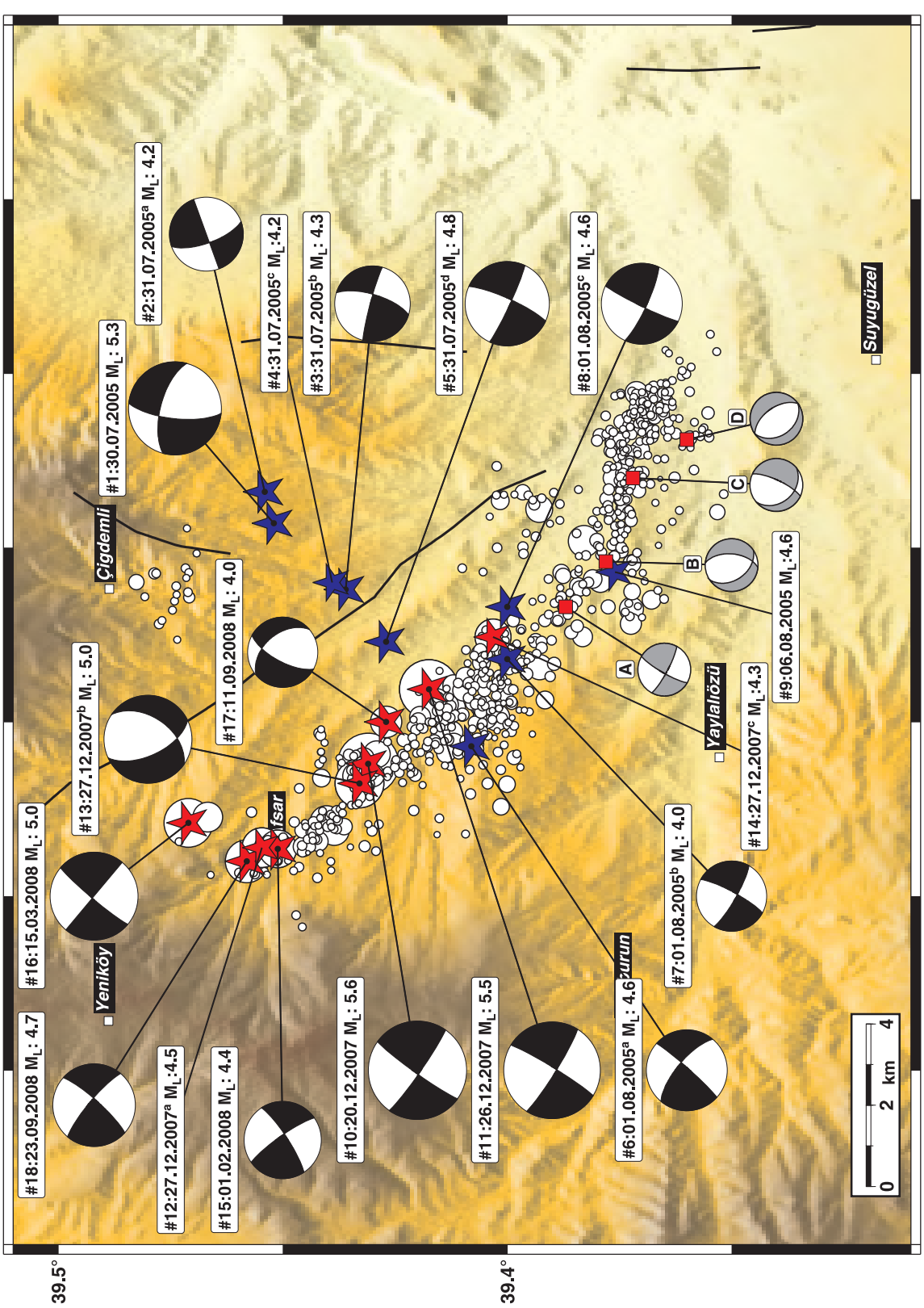

Figure 8. Fault plane solutions, in lower hemisphere projection, of the Bala earthquakes ($M_L \geq 4.0$). The event dates and magnitudes are given above the focal spheres (see Table 6). The epicentres of 2005 and 2007–2008 earthquake sequences are shown as blue and red, respectively. Small focal spheres (in grey) are joint fault plane solution of micro-earthquake groups. Compressional quadrants are shaded.

northeastern end of the sequence. The other three events (#3, #4 and #5) are located between the mainshock and 2007 activity. If the direction of the locations is considered, the focal mechanism solutions indicate NE–SW sinistral strike-slip faulting in 2005 (Koçyiğit 2009). However, there is no more data to confirm this. The other aftershocks of August 1, 2005 (#6, #7 and #8) are located in the same cluster as the 2007 sequence, and might have occurred on a NW–SE dextral strike-slip fault.

The fault plane solutions of the December 20, 2007 Bala earthquake (#10) and its large aftershocks align NW–SE and suggest right-lateral strike-slip faulting. One of the interesting points is that the latest large aftershocks (#12, #15, #16 and #18) are located in the northern segment of the cluster. However, the largest aftershock (#11:26.12.2007, M_L= 5.5) occurred at the junction of the 2005 and 2007 activities. The relatively scattered aftershock distribution in this area may be caused by these conjugate earthquake activities, sourced from the conjugate faulting mentioned by Koçyiğit (2009). Large aftershock activities did not occur south of this point, except for event #14 which has no reliable solution. We also found two normal fault mechanisms with strike-slip component. If right-lateral motion is considered, the December 27, 2007 (#13, M_L= 5.0) and September 11, 2008 (#17, M_L= 4.0) events show SW and NE-dipping planes respectively. The events may be caused by local extensional forces between strike-slip fault segments. Unfortunately, there are no sufficiently large events to allow faulting mechanism in the southernmost segment to be understood. Therefore, we selected closer micro-earthquakes to try to find joint fault plane solutions. The four small groups of events have similar P-wave polarities and give reliable solutions (Table 6, Figure 8). While Group A has strike-slip mechanism, groups B, C and D show normal faulting which indicates extension in this part of the region.

The length of the TGFZ and its unknown historic seismic activity raises the question of future earthquake hazard along the fault, because of the nearby Bala earthquakes. These earthquakes may be considered too small to trigger activity on the neighbouring fault segments. However, King *et al.* (1994) pointed out that increases of Coulomb stress of less than 1 bar sometimes appear to be sufficient to trigger events, depending on the stress level of the fault segments to be triggered. Thus, we tried to calculate the static Coulomb stress changes to understand the relation between the mainshock and the aftershocks. Because of the uncertainties of the 2005 earthquake sequence mentioned in the previous sections, we only analyzed the December 20, 2007 earthquake and its large aftershocks. The stress changes were calculated on specific faults because there was no reliable information for the direction and magnitude of the regional stress field. The average fault plane parameters (strike 130°, dip 80°, rake 180°) from the solutions given in Table 6 was used as the orientation of the specific faults at the calculation grid points and the locking depth was chosen as 5 km. The Coulomb stress change of the December 20, 2007 mainshock is shown in Figure 9A. The four lobes of increased stress rise were observed at the ends of the ruptured segment. The distribution of the aftershocks agrees well with this pattern. Most of them occur on the ruptured segment because unknown details of the fault geometry and slip distribution affect stress change in areas closer to the fault, as mentioned by King *et al.* (1994). The southernmost cluster, which shifts to the east according to the general distribution, occurred completely in the Coulomb stress rise lobe. The small cluster observed near Çiğdemli village may also be explained by the stress rise after the mainshock.

Due to the similar faulting mechanisms and orientations, the cumulative Coulomb stress change of the all aftershocks in 2007 and 2008 do not greatly differ from that of the mainshock (Figure 9B); only the magnitudes of stress rise/fall change. The rate of this magnitude change (< 0.01 bar) is dominant in the NW and the direction of the stress rise lobe in the SE probably indicates that the Bala earthquakes cannot lead to stress increase on the Tuz Gölü Fault Zone (TGFZ), because the Bala fault zone is not the northwestern continuation of the Tuz Gölü Fault Zone.

Discussion

The earthquake area is located near the boundary between the Kırşehir block and the Sakarya

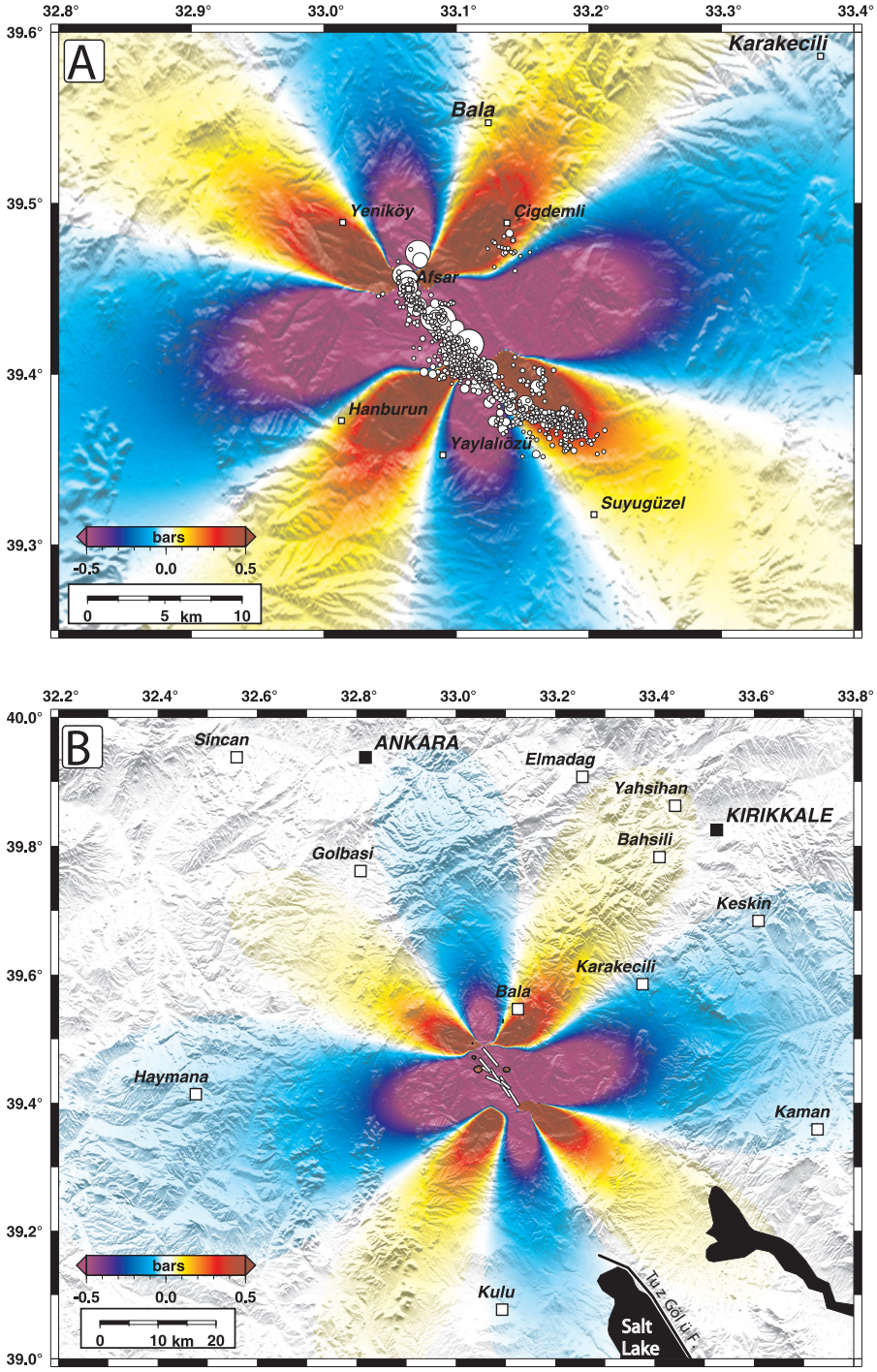

Figure 9. The Coulomb stress change analyzes for the Bala earthquakes on specific faults (strike 130°, dip 80°, rake 180°) at a locking depth of 5 km. **(A)** The relationship between the Coulomb stress change of the December 20, 2007 mainshock and its aftershocks (white circles). **(B)** The cumulative effect of the all large events ($M_L \geq 4.0$) in the Bala region in 2007 and 2008. The white lines are ruptured segments used in the calculations and their lengths are proportional to *L* in Table 6. The stress rise and drop areas are in red and blue, respectively. The contours of stress change values are labelled in bars.

Continent which palaeomagnetic data indicate rotates anticlockwise. Geological field observations show that the N–S contractional neotectonic regime initiated in the Late Pliocene (Koçyiğit & Deveci 2008; Koçyiğit 2009) causes several conjugate faults which have surface rupture tens to hundreds of km long. Following the 1999 İzmit (M_w= 7.4) and Düzce (M_w= 7.2) earthquakes, postseismic motions broadly distributed around coseismic ruptures and increased the stress transfer to within Anatolia. One of the attributes of the stress transfer is seen in the GPS data. Resolvable postseismic changes, by GPS time series, to the velocity field extend at least as far east as the location of the continuous GPS station in Ankara, 200 km SE of the rupture of the devasting İzmit 1999 earthquakes in the Marmara region of Turkey. Seven years after the earthquake sequence, deviations from the interseismic velocity field decreased to ~3 mm/yr (~15% of pre-earthquake motion rate) at Ankara (Ergintav *et al.* 2009). Another attribute comes from the increasing seismological activity at the same time. Especially, NW–SE-trending earthquake activity was observed between the NAFS and Ankara after the 1999 earthquakes. Figure 10 shows the seismic activity in the study area before and after the devastating 1999 earthquakes of İzmit (17.08.1999, M= 7.4) and Düzce (12.11.1999, M= 7.2); the black and yellow dots depict the earthquakes with M ≥ 3.0 occurring before and after the 1999 earthquakes, respectively. The increase in the number of M ≥ 3.0 earthquakes in the study area following the 1999 earthquake sequence is interpreted to be the result of stress transfer to the east with time. The largest event is the June 6, 2000 Orta-Çankırı earthquake (M_w= 6.0), which shows N–S-trending left-lateral strike-slip faulting at shallower depths due to the NW–SE-directed operation of the principal compressive stress around the NAFS (Koçyiğit *et al.* 2001), but becomes N–S normal faulting at greater depths owing to the variation in fault geometry with depth, noted by both seismological and InSAR observations (Taymaz *et al.* 2007; Çakır & Akoğlu 2008). A few events (M ≥ 4.0) have also occurred in Ankara and Çankırı provinces since 2000. These datasets indicate that the deformation of the Anatolian block in this area causes moderate size earthquakes in weak deformation areas such as conjugate fault zones (Afşar and Balaban-Küredağ fault zones in Figure 1B), especially since the stress changes following the two large earthquakes in 1999.

The location and faulting properties of both the 2005 and 2007 earthquake activities near the town of Bala (Ankara, Turkey) seem to hold a key in understanding the regional deformation. Based on both aftershock distribution pattern and field geological mapping data, the fault plane of the July 30, 2005 (M_L= 5.3) earthquake seems most probably NE–SW (NE-trending Balaban-Küredağ left-lateral strike-slip fault zone). However, with better seismological data for the December 20, 2007 (M_L= 5.6) earthquake we are certain that that earthquake occurred on a NW–SE fault segment (NW-trending Afşar Fault Zone). However, the shifting pattern of aftershocks shows approximately E–W extension in the southernmost end of the activity due to the N–S oblique-slip normal faulting component of the major strike-slip faulting. The fault plane solutions agree well with the conjugate faulting pattern, including the NW-trending dextral strike-slip faulting, NE-trending sinistral strike-slip faulting and N–S-trending oblique-slip normal faulting. This also fits well with the strike-slip fault pattern obtained from geological mapping in and around Bala (Figure 1B). The cumulative stress change indicates that there is a risk of the next destructive earthquake occurring in the north, where most of the large aftershocks also occurred. In contrast, the stress increase is small on the Tuz Gölü Fault Zone. Because the national seismology networks cannot observe the micro-earthquake activity (M<2.0–2.5) in the region, it is not possible to confirm whether the TGFZ is seismically active or an inactive fault.

Conclusions

In this study, the location and faulting properties of both the 2005 and 2007 earthquake activities near the town of Bala (Ankara, Turkey) are analyzed in more detail to understand the deformation in the region. The analyses show that the 2005 and 2007 Bala earthquakes may result from increasing stress after the 1999 earthquakes on the NAFS, and mark the present crustal deformation in the Anatolian platelet.

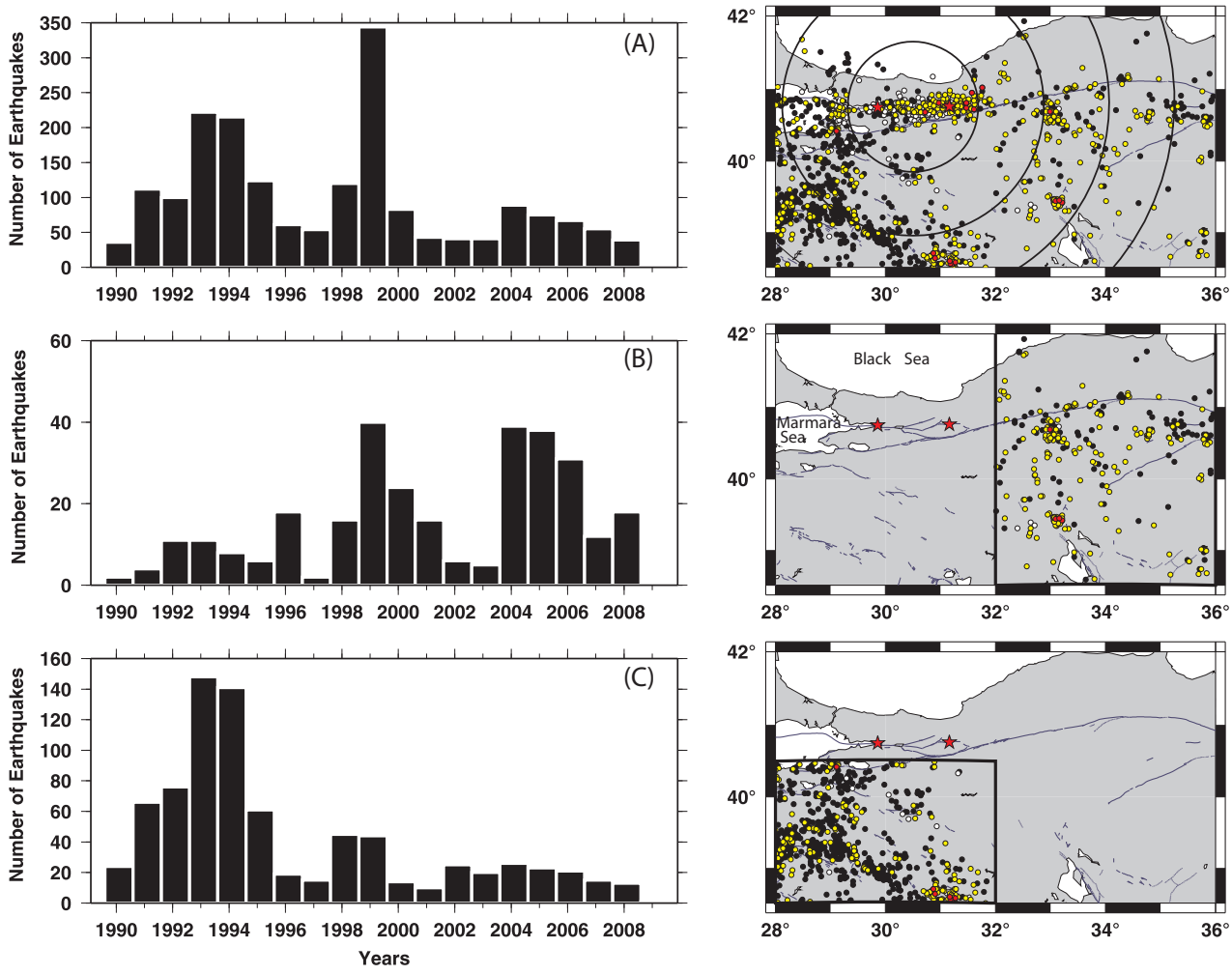

Figure 10. Seismicity in and around the study area before and after the devastating 17 August 1999 (M= 7.4) and 12 November 1999 (M= 7.2) earthquakes (USGS-NEIC, M ≥ 3.0). **(A)** Seismicity in the region covering the epicentral areas of these big earthquakes (red stars) and the nearby areas including the study area (Bala). The circles depict the circular distances of 100, 200, 300, 400 km from the deformation zone related to these big earthquakes. **(B)** Seismicity in the study area, **(C)** Seismicity in the southern part of the epicentral areas of the 1999 earthquakes. Black dots are earthquakes before 17 August 1999 earthquake. White dots are earthquakes occurring between 17 August and 12 November 1999 earthquakes. Yellow dots depict earthquakes occurring after 12 November 1999. The large events (M ≥ 5.0) are shown with red dots. Note the noticeable increase in yellow dots in the study area; suggesting increase of deformation (e.g., transfer of stress from the west to the east by years) in the study area.

The fault plane solutions, the aftershock distributions and the fault pattern show that the main deformation zones trend in NW–SE and NE–SW directions, with many different moderate size fault concentrations causing a series of $M_L \geq 5$ earthquakes.

Based on the Coulomb models and also the epicentral distribution of aftershocks, the main stress increase is northwestwards (towards Ankara; the capital city of Turkey). So, continuous monitoring of this area plays an important role in understanding the behaviour of stress changes in the area.

Acknowledgement

This project (DEPAR – Urgent Monitoring Studies After Earthquake) was supported by the State Panning Organization (DPT) of Turkey and TÜBİTAK Marmara Research Center. We thank Orhan Tatar for his suggestions. The maps and graphs were drawn using the Generic Mapping Tool (GMT) (Wessel & Smith 1991).

References

Aydemir, A. 2009. Tectonic investigation of Central Anatolia, Turkey, using geophysical data. *Journal of Applied Geophysics* **68**, 321–334.

Aydemir, A. & Ateş, A. 2006. Structural interpretation of the Tuzgölü and Haymana basins, Central Anatolia, Turkey, using seismic, gravity and aeromagnetic data. *Earth Planets Space* **58**, 951–961.

Beekman, P.H. 1966. Hasan Dağı–Melendiz Dağı bölgesinde Pliosen ve Kuvaterner volkanizma faaliyetleri [Pliocene and Quaternary volcanism in Hasan Dağı-Melendiz Dağı region]. *MTA Bulletin* **66**, 88–103 [in Turkish with English abstract]

Bozkurt, E. 2001. Neotectonics of Turkey - a synthesis. *Geodinamica Acta* **14**, 3–30.

Çakır, Z. & Akoğlu, A.M. 2008. Synthetic aperture radar interferometry observations of the M= 6.0 Orta earthquake of 6 June 2000 (NW Turkey): reactivation of a listric fault. *Geochemistry, Geophysics and Geosystems* **9**, Q08009, doi:10.1029/2008GC002031.

Çemen, İ., Göncüoğlu, M.C. & Dirik, K. 1999. Structural evolution of the Tuz Gölü basin in Central Anatolia, Turkey. *The Journal of Geology* **107**, 693–706.

Dirik, K. & Göncüoğlu, M.C. 1996. Neotectonic characteristics of Central Anatolia. *International Geology Reviews* **38**, 807-817.

Emre, Ö., Doğan, A., Özalp, S., Yildirim, C. & Albayrak, H. 2005. *31 Temmuz 2005 Bala Depreminin Değerlendirilmesi Raporu [Preliminarily Report of July 31, 2005 Bala Earthquake]*. MTA Report [in Turkish, unpublished].

Ergin, M., Özalaybey, S., Aktar, M., Biçmen, F., Tapirdamaz, M.C., Yörük, A., Tarancioğlu, A., Belgen, A., Yüce, H., Erkan, B. & Yakan, H. 2003. *The Seismicity of Trona Base in Kazan*. TÜBİTAK MRC Earth and Marine Sciences Institute, Research Project Report, no. **5037101** [unpublished].

Ergintav, S., McClusky, S., Hearn, E., Reilinger, R., Çakmak, R., Herring, T., Özener, H., Lenk, O. & Tari, E. 2009. Seven Years of postseismic deformation following the 1999, M= 7.4, and M= 7.2, İzmit-Düzce, Turkey earthquake sequence. *Journal of Geophysical Research* **114**, B07403, doi:10.1029/2008JB006021.

Fréchet, J. 1985. *Sismogenèse et doublets sismiques.* Thèse d'Etat, Université Scientifique et Médicale de Grenoble.

İnan, S., Ergintav, S., Saatçilar, R., Tüzel, B. & Iravul, Y. 2007. Turkey makes major investment in earthquake research. *EOS* **88** (34), 333–334.

Goldstein, P., Dodge, D., Firpo, M. & Ruppert, S. 1998. What's new in SAC2000: enhanced processing and database access. Invited contribution in *Seismological Research Letters* **69**, 202–205.

Got, J.L., Frechet, J. & Klein, F.W. 1994. Deep fault plane geometry inferred from multiplet relative relocation beneath the south flank of Kilauea. *Journal of Geophysical Research* **99**, 15375–15386.

Görür, N., Okay, F.Y., Seymen, İ. & Şengör, A.M.C. 1984. Palaeotectonic evolution of the Tuzgölü Basin complex, central Turkey: sedimentary record of a Neo-Tethyan closure. *In*: Dixon, J.E. & Robertson, A.H.F. (eds), *The Geological Evolution of the Eastern Mediterranean*. Geological Society of London, Special Publications **17**, 467–482.

Gürsoy, H., Piper, J.D.A., Tatar, O. & Mesci, L. 1998. Palaeomagnetic study of the Karaman and Karapınar volcanic complexes, central Turkey: neotectonic rotation in the south-central sector of the Anatolian Block. *Tectonophysics* **299**, 191–211.

Kalafat, D., Kekovali, K., Garip, P., Bekler, F., Gümüş, H., Küsmezer, A., Güneş, Y. & Berberoğlu, A. 2005. *31 July 2005 Bala-Ankara Earthquake Activity*. Preliminary Report, B.U. Kandilli Observatory & ERI, National Earthquake Monitoring Centre, İstanbul, Turkey [unpublished].

King, G.C.P., Stein, R.S. & Lin, J. 1994. Static stress changes and the triggering of earthquakes. *Bulletin of Seismological Society of America* **84**, 935–953.

Kissling, E., Ellsworth, W.L., Eberhart-Phillips, D. & Kradolfer, U. 1994. Initials reference model in local earthquake tomography. *Journal of Geophysical Research* **99** (B10), 19635–19646.

Koçyiğit, A. 2009. Ankara'nın depremselliği ve 2005–2007 Afşar (Bala-Ankara) depremlerinin kaynağı [Seismicity of Ankara and source of 2005–2007 Afşar (Bala-Ankara) earthquakes]. *Harita Dergisi* **141**, 1–12 [in Turkish with English abstract].

Koçyiğit, A. & Beyhan, A. 1998. A new intracontinental transcurrent structure: the Central Anatolian Fault Zone, Turkey. *Tectonophysics* **284**, 317– 336.

Koçyiğit, A. & Devecí, Ş. 2008. Ankara orogenic phase, its age and transition from thrusting-dominated palaeotectonic period to the strike-slip neotectonic period, Ankara (Turkey). *Turkish Journal of Earth Sciences* **17**, 433–459.

Koçyiğit, A., Rojay, B., Cihan, M. & Özacar, A. 2001. The June 6, 2000 Orta (Çankırı, Turkey) earthquake: sourced from a new antithetic sinistral strike-slip structure of the North Anatolian Fault System, the Dodurga fault zone. *Turkish Journal of Earth Sciences* **10**, 69–82.

Lienert, B.R.E. & Havskov, J. 1995. A computer program for locating earthquakes both locally and globally. *Seismological Research Letters* **66**, 26–36.

Lin, J. & Stein, R.S. 2004. Stress triggering in thrust and subduction earthquakes, and stress interaction between the southern San Andreas and nearby thrust and strike-slip faults. *Journal of Geophysical Research* **109**, B02303, doi:10.1029/2003JB002607.

Mai, P.M. & Beroza, G.C. 2000. Source scaling properties from finite-fault-rupture models. *Bulletin of Seismological Society of America* **90**, 604–615.

McClusky, S., Balassanian, S., Barka, A., Demir, C., Ergintav, S., Georgiev, I., Gürkan, O., Hamburger, M., Hurst, K., Kahle, K., Kastens, K., Kekelidze, G., King, R., Kotzev, V., Lenk, O., Mahmoud, S., Mishin, M., Nadariya, M., Ouzounis, A., Paradissis, D., Peter, Y., Prilepin, M., Reilinger, R., Sanli, I., Seeger, H., Tealeb, A., Toksöz, M.N. & Veis, G. 2000. Global Positioning System constrains on plate kinematics and dynamics in the Eastern Mediterranean and Caucasus. *Journal of Geophysical Research* **105** (B3), 5695–5719.

Platzman, E.S., Tapirdamaz, C. & Sanver, M. 1998. Neogene anticlockwise rotation of central Anatolia (Turkey): preliminary palaeomagnetic and geochronological results. *Tectonophysics* **299**, 175–189.

Piper, J.D.A., Gürsoy, H. & Tatar, O. 2002. Palaeomagnetism and magnetic properties of the Cappadocian ignimbrite succession, central Turkey and Neogene tectonics of the Anatolian collage. *Journal of Volcanology and Geothermal Research* **117**, 237–262.

Piper, J.D.A., Tatar, O., Gürsoy, H., Koçbulut, F. & Mesci, B.L. 2006. Palaeomagnetic analysis of neotectonic deformation in the Anatolian accretionary collage, Turkey. *In*: Dilek, Y. & Pavlides, S. (eds), *Postcollisional Tectonics and Magmatism in the Mediterranean Region and Asia*. Geological Society of America Special Paper **409**, 417–440.

Reilinger, R.E., McClusky., S., Oral, M.B., King, R.W. & Toksöz, M.N. 1997. Global Positioning System measurements of present-day crustal movements in the Arabia-Africa-Eurasia plate collision zone. *Journal of Geophysical Research* **102** (B5), 9983–9999.

Şaroğlu, F., Emre, Ö. & Boray, A. 1987. *Active Faults of Turkey and Their Seismicities*. MTA Technical Report *no.* **8174** [in Turkish, unpublished].

Şaroğlu, F., Emre, Ö. & Kuşçu, İ. 1992. *Active Fault Map of Turkey*. MTA Publication.

Şengör, A.M.C. 1979. The North Anatolian transform fault: Its age, offset and tectonic significance. *Journal of the Geological Society, London* **136**, 269–282.

Şengör, A.M.C. & Yilmaz, Y. 1981. Tethyan evolution of Turkey: a plate tectonic approach. *Tectonophysics* **75**, 181–241.

Snoke, J.A., Munsey, J.W., Teague, A.G. & Bollinger, G.A. 1984. A program for focal mechanism determination by combined use of polarity and SV/P amplitude ratio data. *Earthquake Notes* **55**, p. 15.

Stein, R.S., Barka, A. & Dieterich, J.H. 1997. Progressive failure on the North Anatolian fault since 1939 by earthquake stress triggering. *Geophysical Journal International* **128**, 594–604.

Tan, O. & Taymaz, T. 2005. Arabistan-Avrasya kıtasal çarpışma bölgesindeki depremlerin benzerlik ilişkileri [Self-similarity of the earthquakes occurred in the Eurasia-Arabia collision zone]. *İTÜ Dergisi* **4**, 105–115 [in Turkish with English abstract].

Tan, O. & Taymaz, T. 2006. Active tectonics of the Caucasus: earthquake source mechanisms and rupture histories obtained from inversion of teleseismic body waveforms. *In*: Dilek, Y. & Pavlides, S. (eds), *Postcollisional Tectonics and Magmatism in the Mediterranean Region and Asia*. Geological Society of America Special Paper **409**, 531–578.

Tatar, O., Piper, J.D.A., Gürsoy, H. & Temiz, H. 1996. Regional significance of neotectonics counterclockwise rotation in Central Turkey. *International Geology Review* **38**, 692–700.

Taymaz, T., Wright, T., Yolsal, S., Tan, O., Fielding, E. & Seyitoğlu, G. 2007. Source characteristics of June 6, 2000 Orta-Çankırı (Central Turkey) earthquake: a synthesis of seismological, geological and geodetic (InSAR) observations, and internal deformation of Anatolian plate. *In*: Taymaz, T. Yilmaz, Y. & Dilek, Y. (eds) *The Geodynamics of the Aegean and Anatolia*. The Geological Society of London, Special Publications **291**, 259–290.

Toda, S., Stein, R. S., Richards-Dinger, K. & Bozkurt, S. 2005. Forecasting the evolution of seismicity in southern California: Animations built on earthquake stress transfer. *Journal of Geophysical Research* **110**, B05S16, doi:10.1029/2004JB003415.

Toksöz, M.N., Kuleli, S., Gürbüz, C., Kalafat, D., Bekler, T., Zor, E., Yilmazer, M., Öğütçü, Z., Schultz, C.A. & Harris, D.B. 2003. Calibration of regional seismic stations in the Middle East with shot in Turkey. *Abstracts, Nuclear Explosion Monitoring: Building the Knowledge Base, 25th Seismic Research Review*, *September 23–25, 2003*, *Tucson, Arizona*.

Waldhauser, F. & Ellsworth, W.L. 2000. A double-difference earthquake location algorithm: method and application to the northern Hayward fault, California. *Bulletin of Seismological Society of America* **90**, 1353–1368.

Wells, D.L. & Coppersmith, K.J. 1994. New empirical relationships among magnitude, rupture length, rupture width, rupture area, and surface displacement. *Bulletin of Seismological Society of America* **84**, 974–1002.

Wessel, P. & Smith, W. 1991. Free software helps map and display data. *EOS Transactions AGU* **72**, 441–461.